Ultra-thin Nanocomposite Membranes for Highly Sensitive Sensors

T. J. Kang[*], E. Y. Jang[*], J. Lee[*] and Y. H. Kim[**]

[*]School of Mechanical and Aerospace Engineering, Seoul National University
[**]School of Mechanical and Aerospace Engineering and the Institute of Advanced Aerospace Technology, Seoul National University, Korea, yongkim@snu.ac.kr

ABSTRACT

Innovative fabrication of compliant and ultra-thin nanocomposite membranes with nanoscale thickness allows an extraordinary sensitivity and dynamic range, which makes them candidates for a new generation of membrane-based sensor arrays. Here we describe a MEMS-compatible fabrication process of multilayered nanocomposite membranes with the thickness of 25 nm and freely suspended over large square openings with the side dimension of 50-500 μm. The nanomembranes are electrically conductive due to the single-wall carbon nanotube (SWNT) interlayers and they show a very low electrical percolation threshold with the critical exponent value of 1.4±0.21. The present free-standing and ultra-thin nanomembranes have potentials for highly sensitive transducers.

Keywords: nanocomposite, membrane, carbon nanotube, polyelectrolyte

1 INTRODUCTION

Highly sensitive membrane-type sensor arrays are critical for prospective devices and demanded for various applications, such as bio-/chemical, pressure, tactile and acoustic sensors [1,2]. To obtain a highly sensitive and robust sensing platform of membrane transducers, achievable thickness and the corresponding properties should be investigated over the choice of materials and the resolution of lithographical technique. The conventional TD (top-down) technologies have limitations when ultra-thin membranes are required for transducers with high sensitivity and large scale integration. Flexural rigidity of membrane is proportional to the third power of thickness and it is directly related to the sensitivity [3].

Multilayer films of organic compounds on solid substrate have been studied for more than 70 years because they allow fabrication of multifunctional molecular assemblies of tailored architectures, and moreover, the thickness of films can be easily controlled with a molecular precision by using BT (bottom-up) technologies [4]. However, for the purpose of high sensitivity and multifunctionality of a membrane-type transducer, the membrane has to be transferred or directly released from a solid substrate. Therefore, the robust and reliable fabrication method of freely suspended nanomembranes faces enormous challenges using the technology available.

Here we report on a MEMS (microelectromechanical systems)–compatible fabrication of freestanding nanomembranes with the integration of TD and BU technologies. Nanomembranes with nanoscale thickness and microscopic lateral dimensions can show extraordinary sensitivities combined with extreme robustness and it will give a breakthrough for applications in membrane-based, highly integrated microsensor technology.

2 EXPERIMENT AND RESULT

2.1 Block Materials and Building Strategy

In recent years, the construction of multilayered nanocomposite films from polyelectrolytes with alternating charge has received much attention due to the high degree of molecular order induced by interlayer electrostatic forces in these systems. The alternating layer-by-layer assembly of polyelectrolytes with opposite charge, often referred to as electrostatic self-assembly (ESA), has been well-established in the past decades for the preparation of ultra-thin polymer films with molecular precision [5]. One of the variety of ESA methods, multilayered films by using spin-assisted layer-by-layer (SA-LbL) assembly have been reported as a favorable method for highly ordered structures and time-efficient process compared with a conventional dipping method [6]. This fabrication method combines the spin-coating technique with conventional LbL assembly, making it more simple, time-efficient and cost-effective.

In the present study, poly(allylamine hydrochloride) (PAH), poly(sodium 4-styrenesulfonate) (PSS) are utilized as the cationic and anionic polymers for structural materials, respectively, and a central layer of SWNTs are sandwiched between polyelectrolyte multilayers for electrical conductivity of nanomembranes. Three types of nanomembranes are prepared with the stacking sequence of $(PAH/PSS)_{10}$ only, $(PAH/PSS)_5$ $PAH/SWNT_5$ $(PAH/PSS)_5$, and $(PAH/PSS)_5$ $PAH/SWNT_{10}$ $(PAH/PSS)_5$ structures along the thickness direction. A droplet of 0.2% PAH solution is dropped on the substrate and rotated for 20 seconds with the rotation speed of 4,000 rpm. The excessive PAH is washing out with pure deionized water and dried by spinning for 20 seconds, which results in the formation of PAH monolayer. And then, in the same manner, 0.2% PSS solution is deposited. The procedure is repeated until the needed number of polymer bilayers is

achieved. To form the conducting layer, a droplet of SWNT dispersed solution with the mass concentration of 0.05 mg/ml in N,N-dimethylformamide is dropped on the substrate and deposited in the same manner. There is also a washing step with pure deionized water at the same spinning conditions.

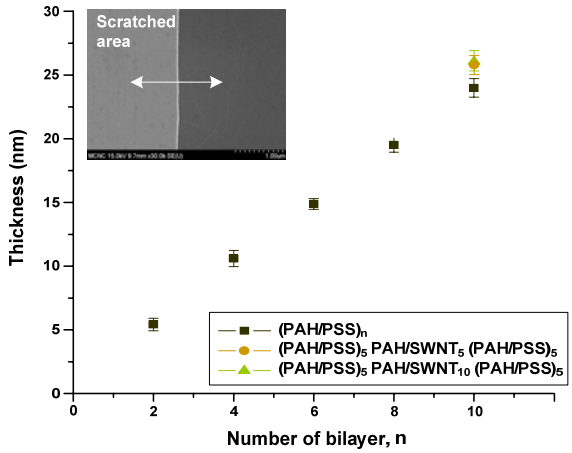

Figure 1: Thickness variation of nanomembranes with the various numbers of polymer bilayers and SWNT layers

The thickness of the nanomembranes can be easily and precisely controlled in the range of single to hundreds nanometer by adjusting the number of polymer bilayers. The increment of 2.4 nm, which represents the average thickness of the bilayer, is determined from AFM measurements. The upper inset of Fig. 1 shows a scanning electron microscopy (SEM) image of the scratched area where the thickness is measured. Figure 1 clearly demonstrates that the thickness of nanomembranes increases linearly with respect to the number of PAH-PSS bilayers. Moreover, the thickness of $(PAH/PSS)_5$ $PAH/SWNT_5$ $(PAH/PSS)_5$ and $(PAH/PSS)_5$ $PAH/SWNT_{10}$ $(PAH/PSS)_5$ structures are measured by 25.78 and 26.05 nm with the standard deviation of 0.75 and 0.86, respectively. The results indicate that SWNT interlayer formed by spin-coating method have a unique morphology of quasi-monolayer and homogeneously distributed on the polymeric layer. Note that the thickness of $(PAH/PSS)_{10}$ structure without SWNT interlayer is 23.99 nm with the standard deviation of 0.73 nm. Distribution and characteristics of SWNT networks will be discussed later.

2.2 Integration of TD and BU Techniques

We have developed a MEMS–compatible fabrication process for nanocomposite membranes with the thickness of 25 nm and freely suspended over large square openings with the side dimension of 50-500 µm. This process includes the integration of TD and BU approaches for reliable and robust fabrication. To utilize the nanomembranes for a transducer, the components of sensor including metal contact, spacer and electrodes are fabricated by using a conventional MEMS process. Fabrication scheme of membrane-based sensors is shown in Fig. 2.

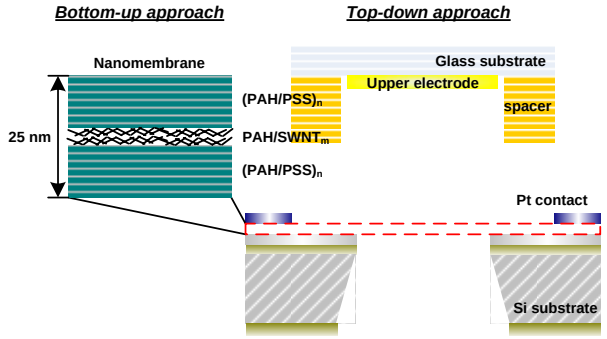

Figure 2: Fabrication scheme of membrane-based sensors

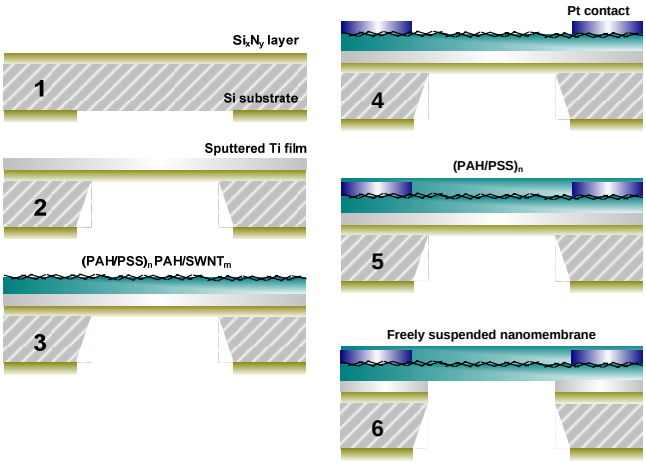

Figure 3: Schematic of the fabrication process

The fabrication process of the free-standing nanomembranes is described in Fig. 3. The process starts with low-stress LPCVD (low pressure chemical vapor deposition) silicon nitride deposition onto cleaned (100)-silicon substrate (see Fig. 3-1), followed by patterning the backside etch holes. Sputtered titanium film is deposited after backside bulk-etching. Thin titanium films as an intermediate layer between the silicon nitride and polymeric layer are utilized for two distinct reasons. One is to provide a hydrophilic surface for spin-coating of polyelectrolyte solution. Hydration property of substrate is one of the most important conditions in the spin-coating method [6], and titanium film is more hydrophilic than silicon nitride film. The other is a protective layer from reactive ion etching of silicon nitride during the releasing process (see Fig. 3-6). Moreover, in the point of etch-selectivity, build-up nanomembranes are safe from the wet-etching of a titanium film. Bottom-side of polymeric multilayer is deposited and SWNT networks are formed by using spin-coating method (see Fig. 3-3). To provide a metal contact, sputtered platinum electrodes are deposited by using shadow mask to exclude a side-effect of photo-lithographical technique such photoresist residue (see Fig. 3-4), and then, upper-side of

polymeric multilayer is deposited (see Fig. 3-5). To release the nanomembranes completely from the substrate, silicon nitride is removed by reactive ion etching, and the titanium film is wet-etched by dilute hydrofluoric acid (see Fig. 3-6).

Figure 4 shows the SEM images of completely released nanomembranes. Utilized polymeric materials are optically transparent, thus a central layer of SWNT networks sandwiched between polyelectrolyte multilayers are clearly shown. SWNT networks are effectively formed and it may be responsible to a low percolation threshold. Moreover, it is confirmed that, as the number of spin-coating increases, the density of SWNT networks increase from Fig. 4-(c) and (d). The released nanomembranes are wrinkle-free as shown in Fig. 4, and independently inspected by optical surface profiler as shown in Fig. 5.

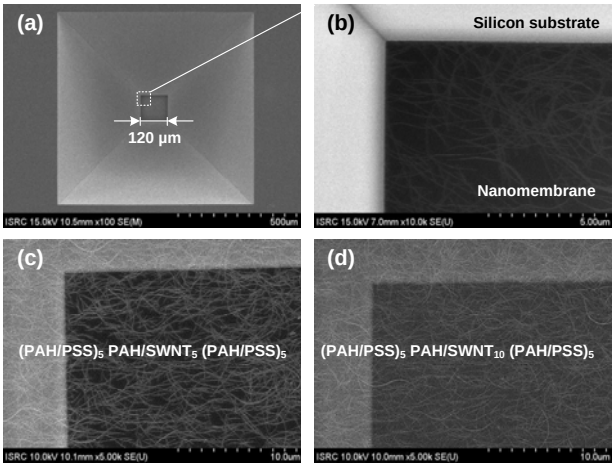

Figure 4: SEM images of released nanomembrane; backside views of (a) and (b), topside views of (c) and (d)

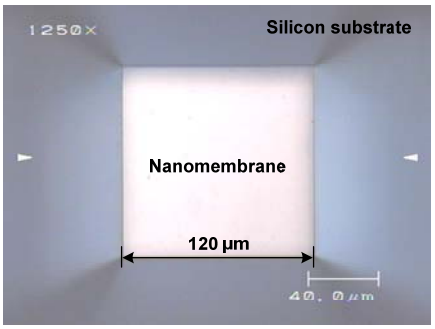

Figure 5: Optical image of wrinkle-free nanomembrane

2.3 Electrical Percolation and Conductivity

To produce uniform networks of SWNT, we utilize spin-coating method that involves centrifugal force, air shear and electrostatic interactions on the polymeric layer. To investigate the effectiveness of spin-coating method and evaluate conductivity in nanomembranes with SWNT networks, the sheet resistances of SWNT networks have been explored by using percolation theory [7], which is adopted to investigate electrical transition and the critical exponent depends on the dimensionality of conducting pathways.

The SWNT networks formed by spin-coating method appear randomly oriented without preferential directions, allowing application of the percolation theory of a random distribution of SWNTs. We prepare a low concentration of the SWNT dispersed solution which has a mass concentration of roughly 1 μg/ml. Several samples are made on the identical glass substrate and polymeric multilayer ($(PAH/PSS)_5PAH$) on it. Conductive networks are formed on the samples with various number of spin-coating of SWNT dispersed solution. After the samples are prepared, a standard four-probe measurement is conducted to measure the sheet resistance (R_s) of SWNT networks. Inset of Fig. 6 shows a plot of sheet conductance σ (defined as $1/R_s$) with respect to the number of spin-coating.

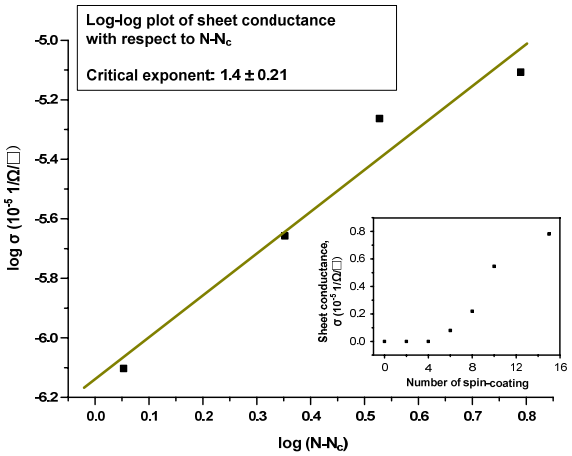

Figure 6: Critical exponent of SWNT networks

The percolation theory predicts that the density dependence of the conductivity is given by

$$\sigma \propto (N - N_c)^{\alpha} \qquad (1)$$

Here, σ refers to the conductance and N is the density of SWNT networks, and N_c is the critical density corresponding to the percolation threshold. The theory predicts the critical exponent of 1.33 for a perfectly two-dimensional film and 1.94 for three-dimensional structures [7].

The average density (SWNTs per area for the number of spin-coating) can be obtained by careful observation of SEM images. The density of SWNT networks with respect to the number of spin-coating can be directly converted into a density of SWNT networks, using the conversion factor of 0.56 (SWNTs/μm^2/spin-coating #). Figure 6 shows a linear curve fitting of measured data in the percolation region. The best fit yields the critical exponent of 1.4±0.21, which is close to the theoretical value of two-dimensional percolation by using a critical density of 2.24 SWNTs/μm^2 at the percolation threshold with the 4 times of spin-coating.

Moreover, it is very simple method for tuning of electrical conductivity and time-efficient. Figure 7 shows a sheet resistance change with respect to the number of spin-coating at the high concentration of 0.05 mg/ml below the critical micelle concentration. Sheet resistance of SWNT networks dramatically decreases and the standard deviation also decreases.

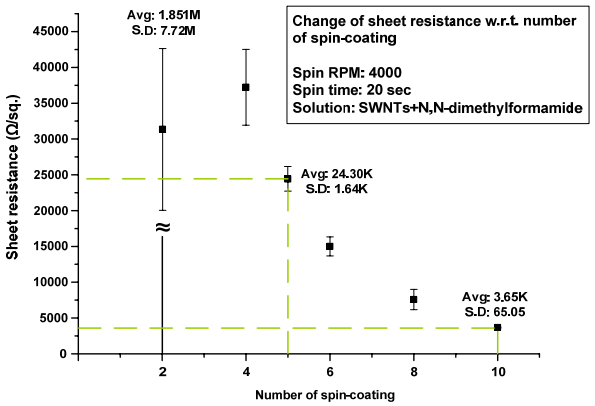

Figure 7: Sheet resistance change with respect to the number of spin-coating

From the result of percolation study in spin-coated SWNT networks, we confirm that spin-coating method to form SWNT networks shows a unique morphology of quasi-monolayer and homogeneously distributed on the polymeric layer. The slight difference between the theoretical value and the measured value is due to the morphology of networks, where SWNTs cross over each other and the randomly distributed junctions between metallic/semiconducting and SWNTs may be responsible to the difference under the presence of the Schottky barriers [8,9].

3 SUMMARY

We fabricate the nanomembranes with the thickness of 25 nm freely suspended over large (hundred micrometres) openings. They are fabricated with molecular precision by spin-assisted layer-by-layer assembly and all the processing steps can be performed with conventional microfabrication facilities. Nanocomposite membranes are composed of multilayered molecular composites combined with polymeric monolayers and SWNTs interlayer. SWNT networks formed by spin-coating show very low electrical percolation threshold with the critical exponent value of 1.4. The present free-standing and ultra-thin nanomembranes can serve as components for a variety of long-lifetime and highly sensitive sensors.

REFERENCES

[1] E. Defay, C. Millon, C. Malhaire, D. Barbier, Sens. Actuators A, 99, 64, 2002.

[2] F. Hedrich, S. Billat, W. Lang, Sens. Actuators A, 84, 315, 2000.

[3] Timoshenko and Woinowski-Krieger, "Theory of Plates and Shells," McGraw-Hill, 180-225, 1970.

[4] Gero Decher, Science, 277, 1232, 1997.

[5] P. Bertrand, A. Jonas, A. Laschewsky, R. Legras, Macromol. Rapid Commun., 21, 319, 2000.

[6] J. Cho, K. Char, J. Hong, K. Lee, Adv. Mater. 13, 1076, 2001.

[7] G. Stauffer, “Introduction to Percolation Theory,” Taylor & Francis, 1985

[8] M. Stadermann, S. J. Papadakis, M. R. Falvo, J. Novak, E. Snow, Q. Fu, J. Lie, Y. Fridman, J. J. Boland, R. Superfin, S. Washburn, Phys. Rev. B, 69, 201402, 2004.

[9] L. Hu, D. S. Hecht, G. Gruner, Nano Lett., 4, 2513, 2004.